An Inelastic Neutron Scattering and NIR−FT Raman Spectroscopy Study of Chloroform and Trichloroethylene in Faujasites

Anne M. Davidson,[†] Caroline F. Mellot,[‡] Juergen Eckert,[§] and Anthony K. Cheetham*

Materials Research Laboratory, University of California at Santa Barbara, California 93106, and Los Alamos National Laboratory, Los Alamos, New Mexico 87545

Received: May 7, 1999; In Final Form: October 21, 1999

Molecular information about the nature and the strength of the interactions between chloroform and trichloroethylene (TCE) sorbates and siliceous FAU, NaY, and NaX zeolites was obtained by inelastic neutron scattering (INS) and Raman spectroscopies. The spectral features of the two sorbates differ in terms of their frequencies, splittings, and line widths from the ones of chloroform and TCE molecules in the gas phase. In conjunction with our simulation results, these differences are rationalized by assuming that, in siliceous FAU, the two sorbates undergo a nondissociative adsorption involving the formation of an $H_{sorbate}\cdots O_{framework}$ hydrogen bond and $Cl_{sorbate}\cdots O_{framework}$ van der Waals interactions, whereas in NaY and NaX, additional $Cl_{sorbate}\cdots Na^+$ electrostatic interactions are involved. Interestingly, no π/Na^+ interaction takes place for TCE. These findings, which are in agreement with previous calorimetric and simulation results, confirm that the strength of the sorbate/zeolite interactions is correlated to the basicity of the zeolite and therefore increases in the sequence siliceous FAU < NaY < NaX, following the sequence of the heats of adsorption.

Introduction

Relatively little information can be found in the literature on the spectroscopic features of hydrohalocarbons in zeolites.[1−4] This is surprising since zeolites are receiving increasing attention because of their ability to adsorb and/or catalytically convert these organics.[5−7] Furthermore, the elimination of halocarbon solvent residues from contaminated waters and soils is an urgent environmental concern,[8] this being especially true for trichloroethylene, TCE, identified as the most abundant pollutant in groundwater in the United States.[9] The main advantage of zeolites, as compared to more conventional separation media such as activated carbons, is that their chemical composition can be adapted to achieve desired separation properties. The hydrophobic/organophilic character of aluminosilicate zeolites can be modulated by adjusting their molar Si/Al ratios (either by preparing high silica polymorphs by synthesis[10a] or by dealumination procedures[10b]). Moreover, for a given molar Si/Al ratio, their acidic/basic character can be fine-tuned through cation exchange that can modify the basicity of framework oxygens.[11]

In an earlier study, we have developed a force field to study the behavior of chloroform in NaY. Computer simulations predicted hydrogen bonding between the weakly acidic proton of chloroform and the basic oxygens of the zeolite, the presence of which was confirmed by inelastic neutron scattering (INS) and Raman methods.[4] More recently, the same force field was used to explain the thermodynamics of chloroform and TCE adsorptions in siliceous FAU, NaY, and NaX.[12,13] The structural features of the binding sites accessible at room temperature, which are not easily accessible to diffraction techniques because of their inherent disorder, were predicted.

In the present contribution, INS and NIR−FT Raman spectroscopy are applied to further characterize, at a molecular level, chloroform and TCE guests within the same series of zeolites. Key features and trends of the modifications of the host/guest interactions as a function of Si/Al ratio and cation contents are addressed.

Experimental Section

Materials. Siliceous FAU, NaY ($Na_{53}Si_{139}Al_{53}O_{384}$), and NaX ($Na_{88}Si_{104}Al_{88}O_{384}$) samples were identical to those used in refs 4, 12, and 13. Since it has been reported that hydrohalocarbons might undergo dissociation on basic zeolites in the presence of residual adsorbed water,[1b] the three zeolites were carefully dehydrated before the introduction of the chloroform and TCE sorbates. No decomposition of the sorbates was detected.

Inelastic Neutron Scattering. Because of the unique sensitivity of neutrons to vibrational modes involving hydrogen atoms, INS is a technique of choice for studying the adsorption of chloroform and TCE within zeolites and for seeking experimental evidence for hydrogen bonding.[14]

The INS data were collected at 25 K using a closed-cycle He refrigerator on the FDS instrument at the Manuel Lujan Jr. Neutron Scattering Center of Los Alamos National Laboratory[15] and were treated after background subtraction by deconvolution of the instrumental response function.[16]

The positions of the INS peaks observed on solid chloroform and TCE (Figures 1a, 2a, respectively) are in close agreement with those already reported from IR and Raman studies in the literature.[17,18] The INS spectra of chloroform and TCE in NaY (Figures 1b, 2b, respectively) and NaX (Figures 1c, 2c, respectively) were measured after loading the dehydrated zeolites (dehydration at 800 K under vacuum) with one molecule

* Corresponding author address: Materials Research Laboratory, University of California at Santa Barbara, Santa Barbara, CA 93106.

[†] Present address: Laboratoire de Réactivité de Surface, UMR CNRS 7609, 4 place Jussieu, 75252 Paris Cedex 05, France.

[‡] Present address: Institut Lavoisier, UMR CNRS 173, Université de Versailles Saint-Quentin, 45 avenue des Etats-Unis, 78035 Versailles Cedex, France.

[§] Los Alamos National Laboratory.

10.1021/jp991515j CCC: $19.00
Published on Web 12/31/1999

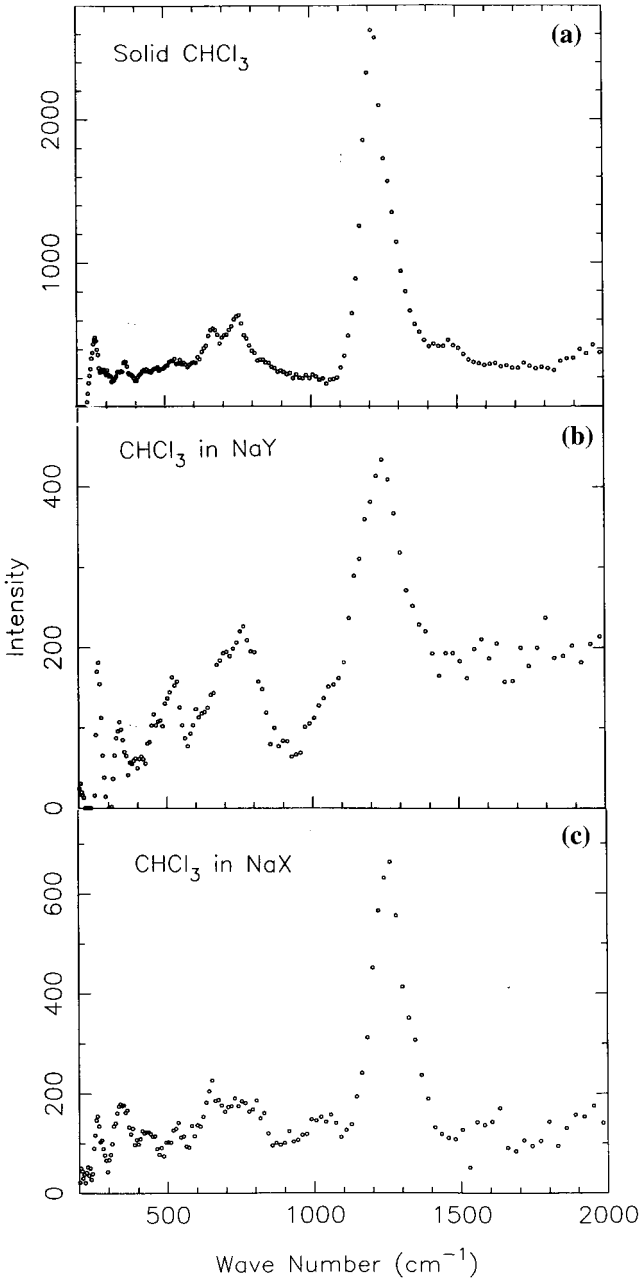

Figure 1. Inelastic neutron scattering spectra at 25 K of (a) solid chloroform; (b) chloroform adsorbed in NaY; (c) chloroform adsorbed in NaX.

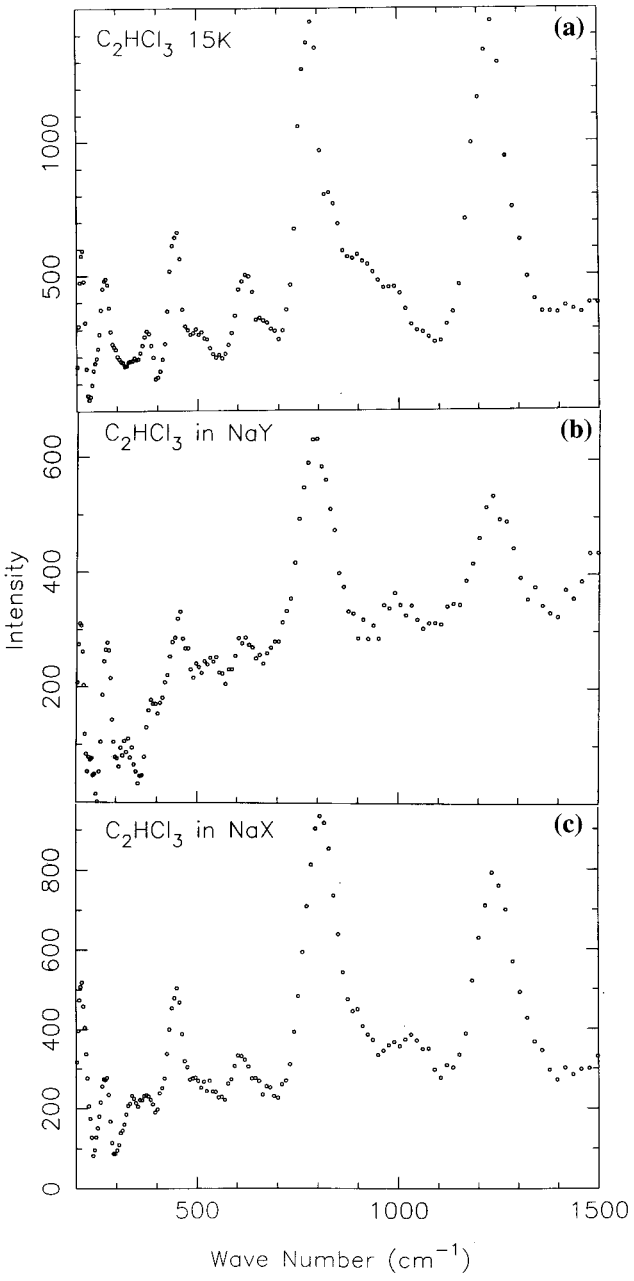

Figure 2. Inelastic neutron scattering spectra at 25 K of (a) solid TCE; (b) TCE adsorbed in NaY; (c) TCE adsorbed in NaX.

of each sorbate per supercage. In these figures the spectra of the dehydrated zeolites have been subtracted.

NIR−FT Raman Scattering. Because of recent advances in NIR−FT instrumentation, Raman spectroscopy is receiving increasing attention for the study of organic guests in zeolites.[4,19] Because of the intrinsically small Raman scattering cross section of inorganic species when compared to that of organic species, the Raman peaks due to sorbate vibrations are easily discriminated from the weak Raman peaks due to the zeolite.[19] The analysis of Raman spectra provides information about the chemical integrity of the sorbates upon adsorption and the nature of the host/guest interactions. Another advantage of NIR−FT Raman spectroscopy as compared to INS is its higher rate of data acquisition, which permits one to follow, in situ, the coverage dependence of the spectra.[4]

Prior to adsorption, the samples were dehydrated at 820 K, using a temperature ramp and hold program [1 °C/min from room temperature to 360 K (2 h), then 390 K (2 h), then 3 °C/min up to 823 K (12 h)] in dry flowing oxygen. The Raman spectra (Figures 3−6) were collected at room temperature (300 K) on an NIR−FT Raman Nicolet 850 spectrometer using an excitation laser with a wavelength of 1064 nm, at low power (typically less than 0.5 W on the sample) and using a 4 cm^{-1} resolution. The Raman cell was made of two independent compartments connected by a valve: one compartment containing the liquid sorbate and the other containing the dehydrated zeolite. At time zero, the connection was opened and the zeolite was exposed to the gaseous sorbate. Raman spectra were collected every 10 min. In a typical data collection, 100−500 scans were added and normalized at each time. After 6 h, no further change in the Raman spectra was observed, which indicates that equilibrium was reached under our experimental conditions (deep bed). The amount of chloroform adsorbed at equilibrium was estimated by gravimetry. One molecule per

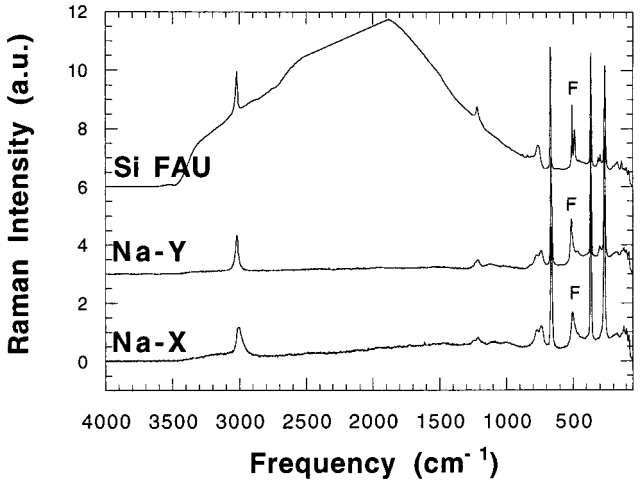

Figure 3. Raman spectra of chloroform in siliceous FAU, NaY, and NaX (spectra collected at room temperature, equilibrium being reached after 2 h).

supercage, on average, was found in the siliceous FAU, 3 in NaY, and 5 in NaX.

The Raman spectra observed at equilibrium for chloroform and TCE adsorption in siliceous FAU, NaY, and NaX are compared in Figures 3 and 5, respectively. The evolutions measured as a function of sorbate loading are presented in Figure 4 for chloroform and in Figure 6 for TCE.

Results and Discussion

All of the vibrations previously identified by others for gaseous chloroform (point group C_{3v}, six independent modes: four nondegenerate and two doubly degenerate[17a]) and TCE (point group C_s, 12 independent and nondegenerate modes[18a]) are observed after their introduction within the zeolites.

Selected vibrational frequencies of chloroform and TCE in siliceous FAU, NaY, and NaX, which can be identified in Figures 3 and 5, are summarized in Tables 1 and 2. These vibrational frequencies were assigned based on previous spectroscopic studies. In the following discussion sorbate frequencies that are hardly affected by adsorption will not be considered. Furthermore, the framework vibrations, which are indicated by symbols F on the figures, will not be discussed. The vibrational frequencies of gaseous chloroform and TCE molecules are used as references to evaluate the frequency shifts associated with the adsorption processes.

Adsorption of Chloroform in Siliceous FAU, NaY, and NaX. *$H_{chloroform}\cdots O_{framework}$ Interactions.* The H−C−Cl bending mode, ν_4, and the C−H stretching mode, ν_1, provide valuable information about the nature and the strength of the interactions between the hydrogen atoms of chloroform and the zeolitic walls.

The doubly degenerate ν_4 mode of chloroform is significantly modified upon adsorption. In the INS spectra (Figure 1) this peak is broadened and shifted upward in frequency in NaY ($\Delta\nu_4 = +27$ cm^{-1}) and in NaX ($\Delta\nu_4 = +29$ cm^{-1}). In the Raman spectra (Figure 3) a single peak is observed in siliceous FAU whose position is nearly identical to that observed for gaseous chloroform ($\Delta\nu_4 = +1$ cm^{-1}). In NaY and in NaX (Figures 3 and 4a) this single peak is split into two distinct contributions, possibly indicating the presence of different adsorption sites or the lowering of symmetry. In line with our previous simulation results[4] and recent spectroscopic results on the adsorption of $CHCl_3$ in cationic faujasites,[20] we believe that the splitting of ν_4 rather arises from the presence of extra framework cations

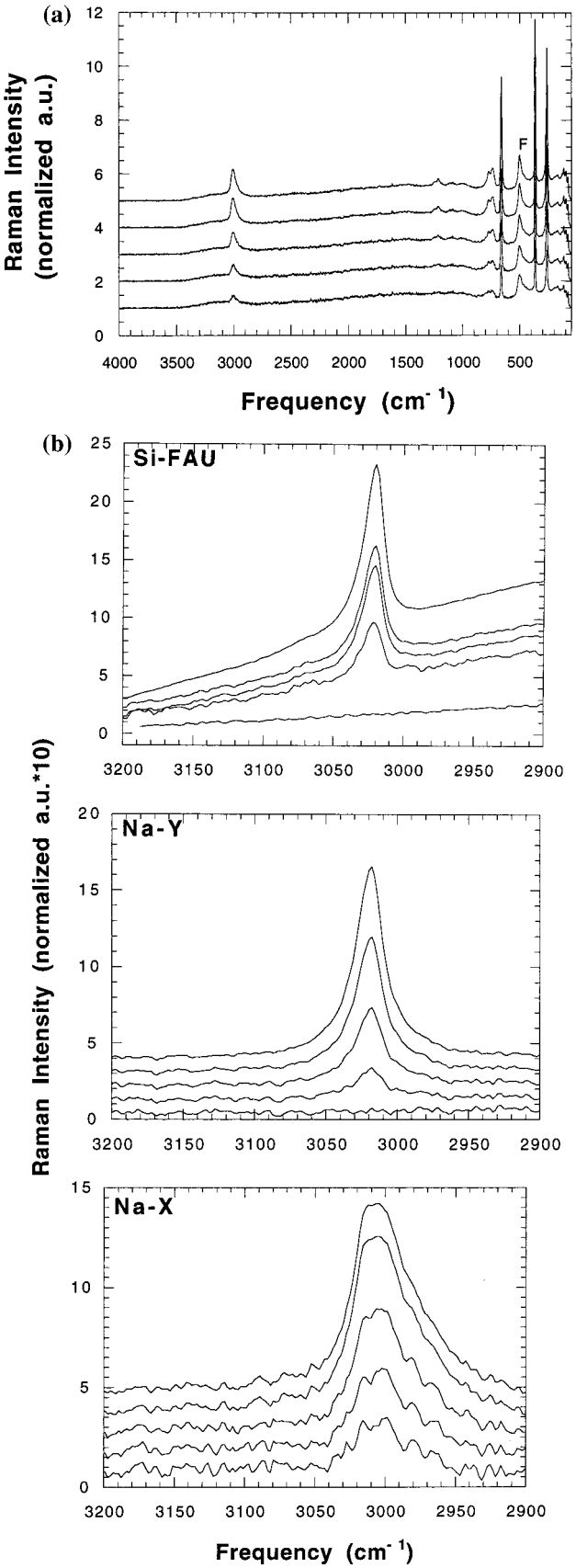

Figure 4. (a) Evolution of the Raman spectra of chloroform in NaX as a function of chloroform loading. (b) Evolution of the C−H stretch of chloroform as a function of the chloroform loading in siliceous FAU, NaY, and NaX.

(Na in sites II and III/III′), generating different local environments of the Cl atoms of the $CHCl_3$ molecules in the 12-ring

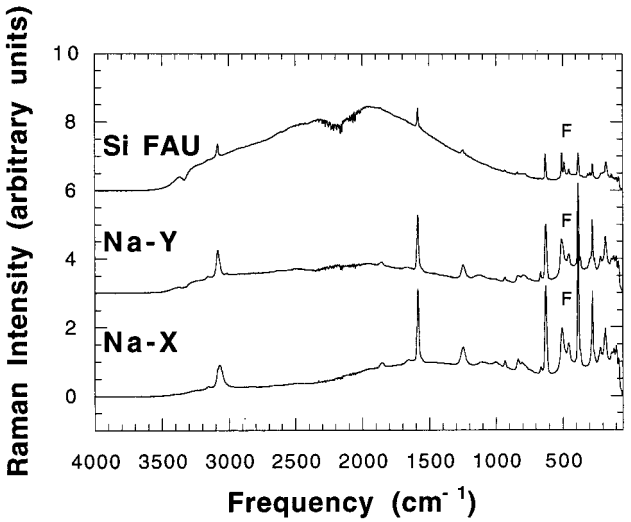

Figure 5. Raman spectra of TCE in siliceous FAU, NaY, and NaX (spectra collected at room temperature, equilibrium being reached after 2 h).

windows. Finally, we have observed that the average position of this doublet is shifted upward compared to siliceous FAU, the shift being smaller in NaY ($\Delta\nu_{4,av} = +2$ cm^{-1}) than in NaX ($\Delta\nu_{4,av} = +9$ cm^{-1}).

The C−H stretching mode, ν_1, as observed by Raman spectroscopy (Figure 4b), is broadened and red-shifted upon adsorption (Table 1). The magnitude of this red shift follows the following sequence: siliceous FAU ($\Delta\nu_1 = -10$ cm^{-1}) < NaY ($\Delta\nu_1 = -12$ cm^{-1}) < NaX ($\Delta\nu_1 = -18$ cm^{-1}). The progressive red shift of the C−H stretch indicates a softening of the C−H bond, which together with the blue-shift of the Cl−C−H bending mode is characteristic of hydrogen bond formation.[21] $H_{chloroform}\cdots O_{framework}$ H-bonds are therefore present in all three systems, and the strength of the H-bonding interactions appears to increase with the basicity of the framework oxygens (siliceous FAU < NaY < NaX).

We also observe in Figure 4b that the peak arising from the C−H stretch, which is symmetrical in NaY, is rather asymmetric in siliceous FAU and even more so in NaX. The asymmetry in the case of NaX may be a consequence of sorbate−sorbate interactions arising from the higher loading of this sample. However, it is also possible that the surface of the zeolite cavities is less homogeneous in the NaX sample because of the disordered distribution of SIII/SIII′ cations. The asymmetric peak shape in siliceous FAU might be attributed to the presence of low levels of silanol defects, or may arise because the configurational energy surface is so smooth that a wide variety of adsorption sites are possible.

Other Interactions. Interactions between the zeolite walls and the Cl atoms of chloroform can be directly probed by studying the evolution of the C−Cl stretching modes, ν_2 and ν_5, upon adsorption. The evolution of the symmetric C−Cl stretching mode, ν_2, is simple. It is not significantly affected in siliceous FAU and it undergoes a downward shift in NaY ($\Delta\nu_2 = -7$ cm^{-1}) and in NaX ($\Delta\nu_2 = -9$ cm^{-1}). This evolution indicates a softening of the C−Cl bonds that we attribute to $Cl_{chloroform}\cdot\cdot\cdot Na^+$ electrostatic interactions.

The evolution of the asymmetric C−Cl stretching mode, ν_5, is discussed on the basis of the Raman spectra since the INS data in this region could be affected by the subtraction of the framework modes which have comparable INS intensity to the C−Cl stretching modes. In the Raman spectrum of siliceous FAU the peak due to ν_5 is blue-shifted ($\Delta\nu_5 = +11$ cm^{-1}), but

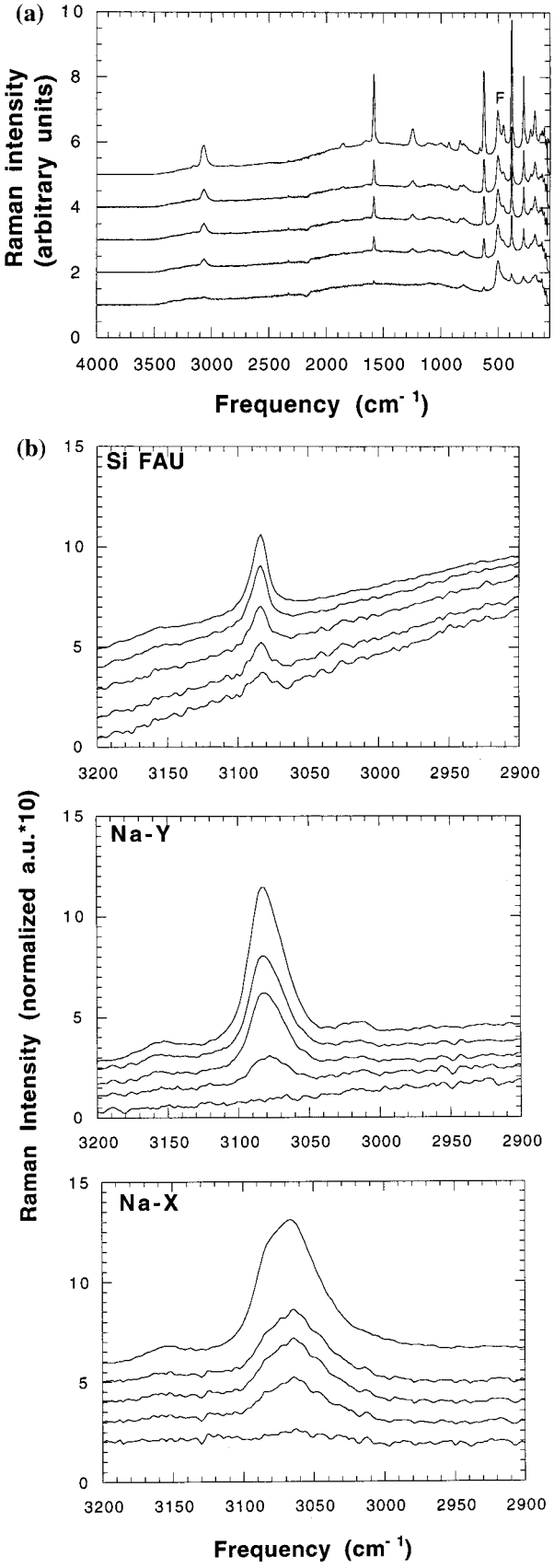

Figure 6. (a) Evolution of the Raman spectra of TCE in NaX as a function of the TCE loading. (b) Evolution of the C−H stretch of TCE as a function of the TCE loading in siliceous FAU, NaY, and NaX.

no splitting is observed. Similarly to the mode ν_4, this mode is split into two contributions in NaY and in NaX, but the average

TABLE 1: Selected Vibrational INS and Raman Frequencies of Gaseous Chloroform, Solid Chloroform, and Chloroform as a Sorbate in Siliceous FAU, NaY, and NaX[a]

		solid	siliceous Y	NaY		NaX	
	gas	INS	Raman	Raman	INS	Raman	INS
mode	ref 17a	(20 K)	(300 K)	(300 K)	(20 K)	(300 K)	(20 K)
$\nu_{1\,(C-H)\ stretch}$	3030		3020	3018		3012	
$\nu_{4\,(H-C-Cl)\ bend}$	1219	1218	1219	1231/1211	1246	1243/1213	1248
$\nu_{5\,(C-Cl)\ stretch}$	760	752	771	775/741	772	772/740	785/735
$\nu_{2\,(C-Cl)\ stretch}$	672	663	669	665	695*	663	652*

[a] The positions of the INS peaks marked by (*) may be affected by the subtraction procedure because of the proximity of framework vibrations.

TABLE 2: Selected Vibrational INS and Raman Frequencies (cm^{-1}) of Gaseous TCE, Solid TCE, and TCE as a Sorbate in Siliceous FAU, NaY, and NaX[a]

		solid	siliceous Y	NaY		NaX	
	gas	INS	Raman	Raman	INS	Raman	INS
mode	ref 18b	(20 K)	(300 K)	(300 K)	(20 K)	(300 K)	(20 K)
$\nu_{1\,(C-H)\ stretch}$	3099		3078	3078		3071	
$\nu_{2\,(C=C)\ stretch}$	1586		1582	1582		1585	
$\nu_{3\,(CH)\ bending}$	1251	1235	1250*	1239	1238	1249	1241
$\nu_{4\,(C-Cl)\ stretch}$	944	~910	926	926		933	
$\nu_{5\,(C-Cl)\ stretch}$	848	~830					
$\nu_{10\,(C-H)\ bending}$	783	776			791		806
$\nu_{6\,(C-Cl)\ stretch}$	631	622	629	626/667(sh)	618*	626/664(sh)	609*

[a] The peak positions marked by a (*) may be imprecise either due the subtraction procedure used after collecting the spectra (INS) or to the presence of a strong fluorescence background (Raman).

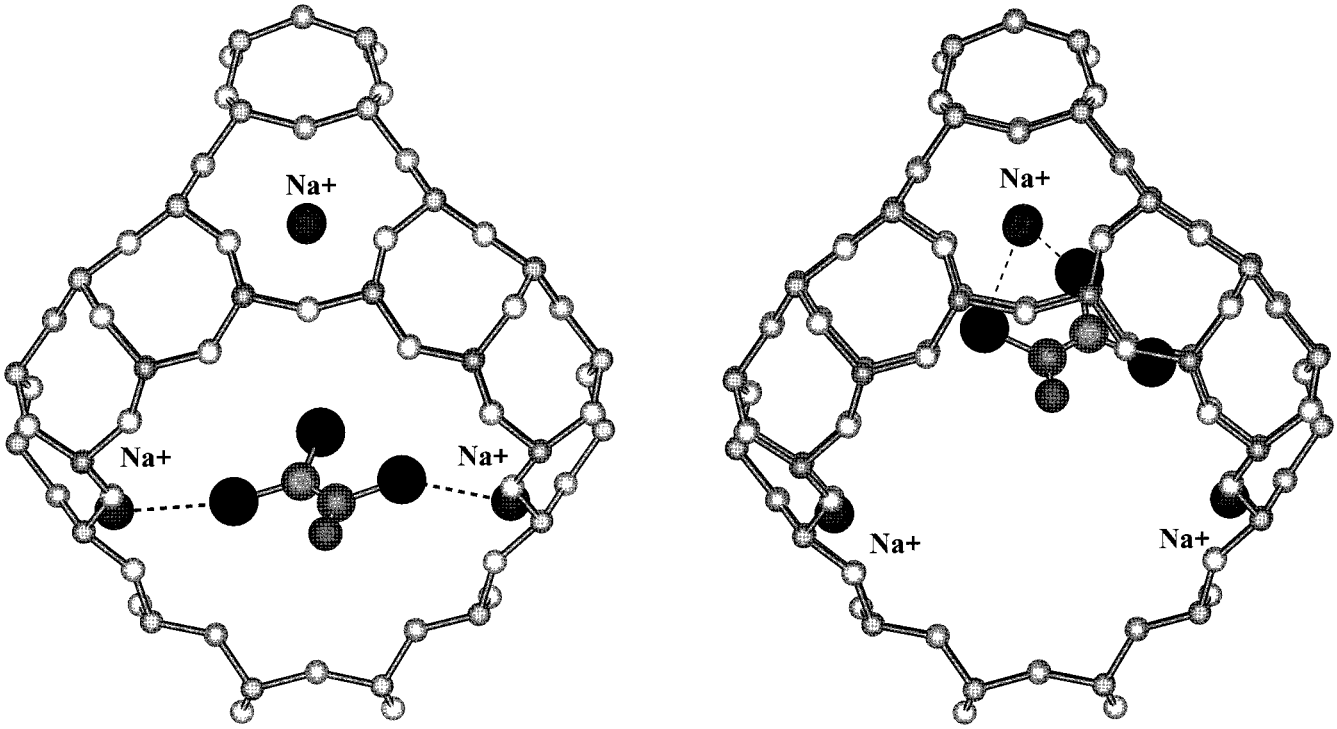

Figure 7. (a) Bridging and (b) bidentate positions of TCE in NaY, as predicted by computer simulations.

frequency remains unchanged from that of gaseous chloroform. These subtle variations may stem from differences in the host−sorbate and sorbate−sorbate interactions in the three sets of experiments.

Adsorption of TCE in Siliceous FAU, NaY, and NaX. *$H_{TCE}\cdots O_{framework}$ interactions.* To explore the possibility that TCE forms hydrogen bonds with the host zeolite we have examined the trends of the ν_1 (C−H stretching), ν_3 (C−C−H and Cl−C−H bending), and ν_{10} (Cl−C−H deformation) modes upon adsorption. In the Raman spectra (Figure 6b) the C−H stretch is strongly red-shifted in siliceous FAU ($\Delta\nu_1 = -21$ cm^{-1}), in NaY ($\Delta\nu_1 = -21$ cm^{-1}), and in NaX ($\Delta\nu_1 = -28$ cm^{-1}) (see Table 2). As in the case of chloroform, the H-bonding between the TCE and the zeolite hosts increases according to the zeolite basicity. From the INS spectra (Figure 2), the two strong peaks, ν_{10} and ν_3, are of particular interest: ν_{10} undergoes a substantial blue-shift both in NaY ($\Delta\nu_{10} = +8$ cm^{-1}) and NaX ($\Delta\nu_{10} = +23$ cm^{-1}), whereas ν_3 shows no significant trend. This behavior may be expected since the displacements of light hydrogen atom for the ν_3 mode are mainly in the plane of the TCE molecule, whereas ν_{10} describes out-of-plane deformations. It is common in hydrogen bonding dynamics for out-of-plane

bending modes to be more sensitive than in-plane bending modes to the presence of hydrogen bonds.[22]

Other Interactions. The observed changes in the C−Cl stretching vibrations, ν_4 and ν_6, are complex and will require more detailed modeling for their interpretation. However, we can draw some interesting conclusions from the changes in the C═C stretching mode, ν_2 (Figure 5, Table 2). In particular, only small shifts relative to the gas phase value are observed ($\Delta\nu_2 < -4$ cm^{-1}), irrespective of the zeolite and the TCE loading. The lack of participation of the C═C double bond during the TCE adsorption in NaY and NaX is especially noteworthy because the analogous mode in ethylene is strongly affected by π/Na$^+$ interactions.[23] Strong electron-donor−acceptor interactions have indeed been observed for ethylene adsorbed on a series of ion-exchanged faujasites,[23] mordenites,[24] and in ZnNaA,[25] where the C═C stretching vibration was detected, respectively, at 1613, 1614, and 1602 cm^{-1}, i.e., significantly lower than that for gaseous ethylene[17] (1623 cm^{-1}). A recent calculation[26] of the internal and external frequencies of ethylene adsorbed in NaY yielded a value of 1596 cm^{-1} for ν_2. The substitution of chlorine atoms in TCE therefore modifies the nature of the interactions of the sorbate with the cation in accordance with our calculations[13] which indicate that the C═C double bond of TCE would not be involved in π/Na$^+$ interactions.

To further probe the binding sites of TCE in these systems in terms of site geometries and host−guest interatomic interactions, we have performed Docking simulations (equivalent to "zero" K calculations) of TCE in NaY for one molecule per unit cell. These were carried out using the so-called Monte Carlo packing procedure,[27] as described in ref 4. A model structure for NaY, $Na_{48}Al_{48}Si_{144}O_{384}$ was built placing the 48 cations in sites I and II. The total host−guest interaction energy was taken as the sum of the short-range term, modeled with a Lennard-Jones potential, and a long-range Coulombic term accounting for the interaction between the dipole moment of the guest and the electrostatic field generated by the zeolite. The short-range contribution was estimated between the zeolite host (oxygen atoms and Na cations) and the TCE molecule (described as a six-site model). Regarding long-range interactions, the zeolite structure was kept rigid and considered as semi-ionic; for circumventing the difficulty of the disordered distribution of Al atoms in the framework, an average T-atom (Al,Si) was considered and its charge chosen to satisfy a Si/Al ratio of 3. Charges of the TCE molecule were estimated from a Hartree−Fock calculation using the 6-31G** basis set, fitting the electrostatic potential surface and scaling the charges so as to give a dipole moment of ∼1.1 D. More details on the derivation of the short-range and long-range parameters used in this work are reported in ref 13. All calculations were carried out using DIZZY[28] with a short-range summation taken up to a cutoff radius of 12 Å and an Ewald summation for the electrostatic term.

The two most favorable binding site geometries found by this simulation are shown in Figure 7. They do not show any host−guest π/Na$^+$ interactions. The first site (the bridging position) shows a TCE molecule located between two Na$^+$ cations in site II, allowing hydrogen bonding, Cl−O and Cl−Na$^+$ interactions. The second site (the bidentate position) shows a TCE molecule adsorbed only near one Na$^+$ cation, still allowing Cl−O and Cl−Na$^+$ interactions. These predictions are broadly consistent with our spectroscopic results. In the future, we intend to perform molecular dynamics calculations of these and related systems in order to probe sorbate mobility and to gain further insight into their vibrational properties.

Conclusions

To the best of our knowledge, this work reports the first INS and Raman spectroscopic studies of chloroform and TCE adsorption in zeolites. In siliceous FAU, NaY, and NaX, the two sorbates participate in a nondissociative mechanism that involves an $H_{sorbate}\cdots O_{framework}$ hydrogen bond. For chloroform, the presence of this hydrogen bond is associated with a red shift of the C−H stretching vibration and a parallel blue shift of the corresponding bending mode. For TCE, this hydrogen bond is indicated by a pronounced blue shift of the out-of-plane CH deformation mode. The hydrogen bonding trends follows the sequence of oxygen basicity: siliceous FAU < Na−Y < Na-X.

For TCE, it is noteworthy that the C═C stretching is not significantly affected upon adsorption in siliceous FAU, Na−Y, or Na-X. Docking simulations confirm that no π/Na interaction takes place. This result is particularly interesting since, in the same zeolites, the double bonds of unsaturated hydrocarbons such as ethylene are found to interact strongly via π interactions with extra framework cations.

Acknowledgment. This work was supported by the United States Department of Energy under grant no. DE-FG03-96ER14672. The Manuel Lujan Jr. Neutron Scattering Center is a national user facility funded by the United States Department of Energy, Office of Basic Energy Sciences−Materials Science, under contract number W-7405-ENG-36 with the University of California. The work made use of facilities supported by the MRSEC Program of the National Science Foundation under Award No. DMR96-32716. A.K.C. thanks the Fondation de l'Ecole Normale Supérieure and the Région de l'Ile de France for a Chaire Internationale de Recherche, Blaise Pascal.

References and Notes

(1) (a) Xie, J. H.; Huang, M. M.; Kaliaguine, S. *React. Kinet. Catal. Lett.* **1996**, *58*, 217. (b) Xie, J. H.; Huang, M. M.; Kaliaguine, S. *Appl. Surf. Sci.* **1997**, *115*, 157.

(2) (a) Chintawar, P. S.; Greene, H. L. *Appl. Catal. B Environ.* **1997**, *14*, 37. (b) Chintawar, P. S.; Greene, H. L. *J. Catal.* **1997**, *165*, 12.

(3) Hannus, I.; Ivanova, I. I.; Tasi, G.; Kiricsi, I.; Nagy, J. B. *Colloids Surf. Sci.* **1995**, *101*, 199.

(4) Mellot, C. F.; Davidson, A. M.; Eckert, J.; Cheetham, A. K. *J. Phys. Chem. B* **1998**, *102*, 2530.

(5) (a) Zarchy, A. S.; Maurer, R. T.; Chao, C. C. U.S. Patent 5,453,-113, 1994. (b) Corbin, D. R.; Mahler, B. A. World Patent, W. O. 94/02440, 1994.

(6) Weber, G.; Bertrand, O.; Fromont, E.; Bourg, S.; Bouvier, F.; Bissinger, D.; Simonot-Grange, M. H. *J. Chim. Phys.* **1996**, *93*, 1412.

(7) George, A. R.; Freeman, C. M.; Catlow, C. R. A. *Zeolites* **1996**, *17*, 466.

(8) (a) Hutchings, G. J.; Heneghan, C. S.; Hudson, I. D.; Talor, S. H. *Nature* **1996**, *384*, 341. (b) Mukhopadhyay, H.; Moretti, E. C. In *Current and Potential Future Industrial Practices for Reducing and Controlling Volatile Organic Compounds*; American Institute of Chemical Engineers, Center Waste Management: New York, 1993.

(9) Westrick, J. J.; Mello, J. W.; Thomas, R. F. *J. Am. Water Works Assoc.* **1984**, *5*, 52.

(10) (a) Alvarez-Cohen, L.; McCarty, P. L.; Roberts, P. V. *Environ. Sci. Technol.* **1993**, *27*, 2141. (b) Kawai, T.; Yanagihara, T.; Tsutsumi, K. *Colloid Polym. Sci.* **1994**, *272*, 1620.

(11) (a) Rabo, J. A. *Catal. Rev. Sci. Eng.* **1981**, *23*, 293. (b) Barthomeuf, D. *Catal. Rev. Sci. Eng.* **1996**, *38*, 521.

(12) Mellot, C. F.; Cheetham, A. K.; Harms, S.; Gorte, R.; Myers, A.; Savitz, S. *J. Am. Chem. Soc.* **1998**, *120*, 5788.

(13) Mellot, C. F.; Cheetham, A. K.; Harms, S.; Gorte, R.; Myers, A.; Savitz, S. *Langmuir* **1998**, *14*, 6728.

(14) Eckert, J. *Physica* **1986**, *136*B, 150; see also in *Spectroscopic Applications of Inelastic Neutron Scattering*; Eckert, J., Kearley, G. J., Eds.; *Special Issue Spectrochim. Acta* **1992**, *48*A.

(15) Taylor, A. D.; Wood, E. J.; Goldstone, J. A.; Eckert, J. *Nuc. Instrum. Methods Phys. Res.* **1984**, *221*, 408.

(16) Sivia, D. S.; Vorderwish, P.; Silver, R. *Nuc. Instrum. Methods Phys. Res.* **1990**, A*290*, 492.

(17) (a) Herzberg, G. In *Molecular spectra and molecular structure*; Van Nostrand: Princeton, 1945, Vol. 2. (b) Devaure, J.; Turrell, G.; van Huong, P.; Lascombe, J. *J. Chim. Phys*. **1967**, 1064. (c) Andrews, B.; Anderson, A.; Torrie, B. *Chem. Phys. Lett.* **1984**, *104*, 65.

(18) (a) Bernstein, H. J.; Allen, G. *Can. J. Research*, **1950**, B*28*, 132. (b) Sverlov, L. M. In *Vibrational Spectra of Polyatomic Molecules*; Wiley: New York, 1974. (c) Phillips, L. A. Raupp, G. B. *J. Mol. Catal.* **1992**, *77*, 297. (d) Fan, J.; Yates, J. T. *J. Am. Chem. Soc.* **1996**, *118*, 4686.

(19) (a) Burch, R.; Passingham, C.; Warnes, G. M.; Rawlence, D. J. *Spectrochim. Acta* **1990**, *2*, 243. (b) Davidson, A.; Weigel, S. J.; Bull, L.; Cheetham, A. K. *J. Phys. Chem.* **1997**, *101*, 3065. (c) Knops-Gerritis, P. P.; De Vos, D. E.; Feijen, E. J. P.; Jacobs, P. A. *Microporous Mater*. **1997**, *8*, 3. (d) Ashtekar, S.; Barries, P. J.; Hargreaves, M.; Gladden, L. F. *Angew. Chem., Int. Ed. Engl.* **1997**, *36*, 376. (e) Hong, S. B.; Camblor, M. A.; Davis, M. E. *J. Am. Chem. Soc.* **1997**, *119*, 761. (f) Borja, M.; Dutta, P. K. *Nature* **1993**, *362*, 43.

(20) Bosch, E.; Huber, S.; Weitkamp, J.; Knozinger, H. *Phys. Chem. Chem. Phys.* **1999**, *1*, 579.

(21) Novak, A. *Struct. Bonding* **1974**, *18*, 177.

(22) Allen, G.; Bernstein, H. J. *Can. J. Chem*. **1954**, *32*, 1044.

(23) Carter, J. L.; Yates, D. J. C.; Lucchesi, P. J.; Elliott, J. J.; Kevorkian, V.; *J. Phys. Chem.* **1966**, *70*, 1126.

(24) Matsuzawa, H.; Yamashita, H.; Ito, M.; Iwata, S. *Chem. Phys.* **1990**, *147*, 77.

(25) Howard, J.; Nicol, J. M.; Eckert, J. The Structure of Surfaces; *Springer Ser. Surf. Sci*. **1985**, *2*, 219.

(26) Henson, N. J.; Eckert, J.; Hay, P. J.; Redondo, A., to be submitted.

(27) Freeman, C. M.; Catlow, C. R. A.; Thomas, J. M.; Brode, S. *Chem. Phys. Lett*. **1991**, *186*, 137.

(28) Henson, N. J.; Auerbach, S. M.; Peterson, B. K. *DIZZY Computational Chemistry Program*; Los Alamos National Laboratory: Los Alamos, NM and University of Massachusetts: Amherst, MA, 1994−1998.